Middle East Journal of Applied Sciences, 4(3): 615-628, 2014
ISSN: 2077-4613

# Utilization of Nano-hydroxyapatite and its Derivatives for Removal of $Fe^{2+}$ from Groundwater at Sohag area, Egypt

**[1]Abo-ElEnein, S.A., [2]Gedamy, Y.R., [2]Hasan, A.A., [3]Khaled, I. and [3]Ecresh, A.**

*[1]Department of Chemistry, Faculty of Science, Ain Shams University, Cairo, Egypt.*
*[2]Hydrogeochemistry Dept., Desert Research Center, El-Matareya, Cairo, Egypt.*
*[3]The Holding Company for Drinking Water and Wastewater, Egypt.*

**ABSTRACT**

The aim of this work is to synthesize and characterize chemically nano-sized powders of hydroxyapatite (HAp), apatitic tricalcium phosphate (TCPa) and apatitic octacalcium phosphate (OCPa) and use them for removal of Fe(II) from aqueous solutions (as groundwater). The sorbents were characterized by Fourier transform infra-red spectroscopy (FT-IR), X-ray diffraction (XRD) and transmission electron microscopy (TEM) analyses. Batch adsorption studies were conducted to optimize various equilibrating conditions like pH, contact time, nano-opowder dosage, initial $Fe^{2+}$ concentration and temperature. The obtained results indicate that the maximum equilibrium $q_e$ values obtained for HAp, TCPa and OCPa nano-powders are 18.68, 18.76 and 16.46mg/g, respectively, for 0.1g dosage and 40mg/L initial Fe(II) concentration at 60°C, pH reaches to 6 and 60min contact time. The TCPa nano-powder showed higher sorption capacity value than those of the HAp and OCPa nano-powders. Isotherm studies indicate that the Langmuir model fits the experimental data better than Freundlich model. Accordingly, synthetic hydroxyapatite (HAp), apatitic tricalcium phosphate (TCPa) and apatitic octa calcium phosphate (OCPa) are very efficient, low cost adsorbents and a promising alternative for eliminating Fe(II) from contaminated waters.

***Keywords:*** Nano-hydroxyapatite, Fe(II) removal, groundwater.

## Introduction

Iron is the second most abundant metal in the earth's crust, and is mainly present in natural water in two oxidation states: Fe(II) and Fe(III). Fe(II), is essential for proper transport and storage of oxygen by means of hemoglobin and myoglobin (Safavi and Abdollahi, 1999). Iron in environmental water comes from steel tempering, coal coking and mining industries (Aksu *et al*., 1999). Noteworthy, the water bearing formation can be consider as one of the sources for Fe(II) in the study area. Water contamination by iron ($Fe^{2+}$) ions is a serious environmental problem, where iron ($Fe^{2+}$) ions can be considered as toxic pollutants that are non biodegradable and have environmental, public health and economic impacts.

The methods used for the removal of heavy metals from water include chemical precipitation (Aydin and Soylak, 2007), ion exchange (Sarzanini *et al*., 2001), solvent extraction (Okamoto *et al*., 2000) and adsorption (Wan *et al*., 2005). Among these methods, adsorption has been proved to be an efficient and economical technique. Activated carbon and silica gel are the two most popular adsorbents (El-Shafey *et al*., 2002) for trace element. But they are relatively expensive materials since the higher the quality, the greater their cost. The use of alternative low-cost materials as potential sorbents for the removal of heavy metals has been emphasized recently.

In this regard, nano-sized powders of hydroxyapatite (HAp), apatitic tricalcium phosphate (TCPa) and apatitic octa calcium phosphate (OCPa) can be used for removal of Fe(II) from aqueous solutions (as groundwater). Apatites with the general formula $Me_{10}(X)_6(Y)_2$, where Me represents divalent cations ($Ca^{2+}$, $Mg^{2+}$), X represents di- or trivalent anions ($PO_4^{3-}$, $CO_3^{2-}$) and Y represents monovalent anions ($OH^-$, $F^-$, $Cl^-$) are the most widespread natural occurring phosphate minerals and the major constituents of bone and vertebra teeth. One of the most interesting properties of apatites is their ability to accept ionic substituents and vacancies. Most exchange reactions concerning nanocrystalline apatites in living beings are related to the exchange of surface ions playing a significant role in homeostasis and in intoxication by mineral (Cazalbou *et al*., 2005). Such exchange reactions are possible due to the very high specific surface area of the hydroxyapatite nanocrystals and because of the existence of a metastable hydrated layer on the crystal surface containing loosely bound ions (Cazalbou *et al*., 2005).So, Calcium hydroxyapatite (HAp), $Ca_{10}(PO_4)_6(OH)_2$, has been used for the removal of heavy metals from contaminated soils and wastewater (Takeuchi and Arai, 1990; Ma *et al*.,1993; Ma *et al*., 1994; Laperche *et al*.,1996; Chen *et al*.,1997; Mavropoulos *et al*., 2002, and Nzihou and Sharrock, 2002). Calcium hydroxyapatite (Ca-HAp) is a principal component of hard tissues and has been of interest in industry and medical fields. Its synthetic particles find many applications in chromatographic adsorbents to separate

**Corresponding Author:** Yahia R. Gedamy, Desert Research Center, El Matariya, Cairo, Egypt.
E-mail: yahiagedamy2014@yahoo.com

protein and enzyme, catalysts for dehydration and dehydrogenation of alcohols, methane oxidation, and as powders for artificial teeth and bones paste germicides (Elliott, 1994). These properties are related to various surface characteristics of HAp, e.g., surface functional groups, acidity and basicity, surface charge, hydrophilicity and porosity. It has been found that Ca-HAp surface possesses 2.6 groups $nm^{-2}$ of P–OH groups acting as sorption sites (Tanaka *et al*., 2005). Hydroxyapatite is an ideal material for long-term containment of contaminants because of its high sorption capacity for actinides and heavy metals, low water solubility, high stability under reducing and oxidizing conditions, availability, and low coast (Krestou *et al*., 2004). The sorption properties of HAp are of great importance for both environmental processes and industrial purposes. It has been reported that the sorption is taking place through ionic exchange reaction, surface complexation with phosphate, calcium and hydroxyl groups and/or co-precipitation of new partially soluble phases. Calcium phosphate, especially apatite's, present remarkable interest due to their availability, structure, ionic exchange property, adsorption affinity, and their ability to establish bonds with heavy metals, have conferred this material to attract more attention.

The objective of this study is to investigate the possible use of nano-crystalline hydroxyapatite, apatitic tricalcium phosphate and apatitic octacalcium phosphate as alternative adsorbents for the removal of $Fe^{+2}$ from aqueous solutions (groundwater). The adsorption models will be used to fit the equilibrium isotherm.

## Materials and Methods

*Materials:*

All chemicals used in this work were of pure and analytical grade and the aqueous solutions were prepared using de-ionized water. Calcium nitrate 4-hydrate [$Ca(NO_3)_2 \cdot 4H_2O$, BDH, England], di-ammonium hydrogen phosphate [$(NH_4)_2HPO_4$, Riedel-de Haën, Germany] and ammonia solution. A synthetic stock solution of $Fe^{2+}$was prepared for the metal ion studies $Fe^{2+}$using its sulfate salt ($FeSO_4.7H_2O$, Merck) in de-ionized water.

*Preparation of nano-crystalline apatite sorbents:*

Hydroxyapatite [$Ca_{10}(PO_4)_6(OH)_2$] nano-powder was prepared by solution-precipitation method (Mobasherpour *et al*., 2007) using calcium nitrate 4-hydrate $Ca(NO_3)_2.4H_2O$ and di-ammonium hydrogen phosphate $(NH_4)_2HPO_4$ as starting materials and ammonia solution as agents for pH adjustment. A suspension of $Ca(NO_3)_2.4H_2O$ (23.61g $Ca(NO_3)_2.4H_2O$ in 350ml distilled water) was vigorously stirred and its temperature was maintained at 25°C. A solution of $(NH_4)_2HPO_4$ (7.92g $(NH_4)_2HPO_4$ in 250ml distilled water) was slowly added drop wise to the $Ca(NO_3)_2.4H_2O$ solution. In all experiments the pH of $Ca(NO_3)_2.4H_2O$ solution by ammonia solution was 11. The precipitated HAp has been removed from solution by centrifugation method at the rotation speed of 3000rpm and was rinsed with water to bring the pH level to 7. The resulting powder was dried at 80°C and then calcined at 100°C for 1h.

Apatitic tricalcium phosphate [$Ca_9(HPO_4)(PO_4)_5(OH)$] nano-powder was prepared by an aqueous precipitation method (Destainville *et al*., 2003) from the addition of a diammonium phosphate solution $(NH_4)_2HPO_4$ to calcium nitrate solution $Ca(NO_3)_2.4H_2O$. Solution A (26g of di-ammonium hydrogen phosphate dissolved in 1300ml of distilled water with addition of 20ml ammonia solution) was added quickly at room temperature to solution B (47g of calcium nitrate 4-hydrate dissolved in 550ml of distilled water with addition of 20ml of ammonia solution).The $(NH_4)_2HPO_4$ addition rate was controlled using a peristaltic pump. The pH value of the solution was maintained at a constant value by the addition of the ammonium hydroxide solution using a pH controller and dosing pump system. The temperature was controlled and regulated. The suspension was continuously stirred and refluxed. After total addition of the $(NH_4)_2HPO_4$ solution, the suspension was ripened from 15 min up to 48 h.Then, the resulted precipitate was filtered (without washing) and dried at 100°C during 24 h.

Apatitic octa calcium phosphate [$Ca_8(PO_4)_4(HPO_4)_2.5H_2O$] nano-powder was also prepared by a fast co-precipitation method (Lebugle *et al*., 1986) between a calcium solution [$A^{/}$] and a basic phosphate solution [$B^{/}$] in an aqueous ethanol solution (50% ethanol by volume).Solution $A^{/}$ (4.92g of calcium nitrate 4-hydrate dissolved in 100ml distilled water with addition of 100ml of ethanol) was immediately poured at 37°C into solution $B^{/}$ (3.96g of di-ammonium hydrogen phosphate in 250ml distilled water with addition to 45ml ammonia solution and 295ml of ethanol). The co-precipitate was filtered off, and then washed with 180ml of distilled water, 30ml of ammonia solution and 210ml of ethanol. It then dried in an oven at 80°C for 24h.

*Identification tools of the adsorbents characterization:*

The resulting powders were subjected to Fourier Transform Infrared analysis (FT-IR, Perkin Elmer, model No. L1600300, UK) with a spectrometer. Infrared spectroscopy IR was carried out after dispersion of the sample

in anhydrous KBr pellets. At first the powdered sample was carefully mixed with KBr (infrared grade) by mixing ratio 1:9 and compressed to form a disk and palletized under vacuum. The IR spectra of the samples were recorded in transmittance mode over a wave No. of range 400 to 4000cm$^{-1}$ at ambient temperature (25ºC).

Powder X-ray diffraction was used to identify the crystalline phases present in the product. The resulting synthesized powders were analyzed by X-ray diffraction (XRD)**,** Philips PW 1170 with Ni filter Cu radiation at 40Kv and SSMA. The samples were scanned at a speed of 2θ/minute (Moore and Reynolds, 1989).

The morphology and particle size of the synthesized adsorbents powders were identified by Transmission Electron Microscopy (TEM, JEM2100, HT:200kv, Magnification: 1.5Max, Resolution: 0.1432nm). For this purpose, particles were deposited onto Cu grids, which support a "holey" carbon film. The particles were deposited onto the support grids by deposition from a dilute suspension in acetone or ethanol. The particles shape and size were characterized by diffraction (amplitude) contrast and, for the crystalline materials, by high resolution (phase contrast) imaging.

*Fe(II) solutions:*

Fe(II) used in this study was obtained as $FeSO_4.7H_2O$ (analytical grade) and used without further purification. The sorption experiments were performed by batch equilibration method. A stock solution of Fe(II) of 1000mg/l was prepared from the pure crystalline solid ($FeSO_4.7H_2O$) in distilled water. All solutions used for sorption experiments were diluted with distilled water as required. The initial concentrations of Fe(II) solutions tested were 10, 20, 30 and 40mg/l. The prepared Fe(II) solutions were stored in brown glass reservoirs to prevent photo-oxidation.

*Methods of adsorption studies:*

The experimental process was carried out by introducing a certain quantity of HAp, TCPa and OCPa nano-powders into three conical flasks, then, a definite volume of Fe(II) solution was added to each flask, vibrated sometime at a constant speed of 240rpm in an air bath mechanical shaker. After a period of shaking (2h) and contact time, the contents of conical flasks, were filtrated to separate HAp, TCPa and OCPa nano-powders from their solutions. The Fe(II) concentration of each filtrate solution was immediately measured using ICP. TheFe(II) adsorption capacity (qe as mg/g) was determined as follows:

$$q_e=(C_0 - C_t)V/m \quad (1)$$

Where; $C_0$ is the initial Fe(II) concentration (mg/L), $C_t$ is the Fe(II) concentration at time $t$ (mg/L), $V$ is the volume (L) of aqueous solution containing Fe(II) and m is the mass of HAp or TCPa or OCPa nano-powder adsorbent (g). The effects of pH (3–6), contact time (10–60min), adsorbent dosage (0.05–0.3g/l), initial concentrationof Fe(II) (10, 20, 30 and 40mg/l) and temperature (20, 40 and 60°C) were studied. Each experiment was repeated three times and the given results were the average values. The initial pH of the working solution was adjusted by 0.1mol/l HCl and 0.1mol/l NaOH solution.

*Adsorption isotherms:*

To investigate the isotherms and equilibrium of Fe(II) adsorption on HAp, TCPa and OPCa nano-powders, a mass of 0.1g of HAp orTCPa or OCPa nano-powder was placed into a conical flask containing 50ml of Fe(II) solution with pH of 6 at various concentrations, and then vibrated at a constant speed of 240rpm using an air bath mechanical shaker for 2h. In order to study the adsorption isotherms, 60min of contact time were used to allow attainment of adsorption equilibrium at a three constant temperatures of 20, 40 and 60°C. After shaking and contacting, the contents of conical flasks, were filtrated to separate HAp, TCPa and OCPa nano-powders from their solutions. The Fe(II) concentration of each filtrate was immediately measured. The Fe(II) adsorption capacity ($q_e$, mg/g) was calculated according to Eq. (1). In the present study, The Langmuir (1918) and Freundlich (1906) models were applied to describe the equilibrium nature of Fe(II) adsorption onto HAp, TCPa and OCPa nano-powders.

**Results and Discussion**

*Characterization of the adsorbents:*

Figure (1) shows the FT-IR spectra of the synthesized adsorbents powders. Characteristic bands exhibited in the samples spectra are as follows; three bands were appeared at 3449, 3572 and 3579cm$^{-1}$ for HAp, TCPa and OCPa, respectively and were due to the stretching mode of hydrogen-bonded $OH^-$ ions. Nine bands were

identified at (873, 604 and 567cm$^{-1}$), (872, 604 and 566cm$^{-1}$) and (874, 601 and 566cm$^{-1}$) for HAp, TCPa and OCPa, respectively and were attributed to the bending mode of phosphorous-oxygen bonded of $PO_4^{3-}$ ions. Carbonate contents ($CO_3^{2-}$ peaks) also were located at (1636 and 1399cm$^{-1}$), (1633 and 1300cm$^{-1}$) and (1634 and 1333cm$^{-1}$) for HAp, TCPa and OCPa, respectively, indicating of the presence of carbonate apatite. This might originate from absorption of carbon dioxide from the atmosphere (Komath and Varma, 2003, and Wei *et al*., 2003). Noteworthy to mention that, there are two stretching bands attributed to the hydrogen-bonded $OH^-$ ions were appeared at 3193 and 3150cm$^{-1}$ for both TCPa and OCPa adsorbents, respectively and no band appeared for HAp adsorbent. Also, two bending bands attributed to the phosphorous-oxygen bonded of $PO_4^{3-}$ions were appeared at 1067 and 1100cm$^{-1}$ for both TCPa and OCPa adsorbents, respectively and no band appeared for HAp adsorbent. The appearance of hydrogen-bonded $OH^-$ ions and phosphorous-oxygen bonded of $PO_4^{3-}$ ions for both TCPa and OCPa adsorbents corresponds to the decrease of the calcium ions in both TCPa and OCPa adsorbents molecules compared to HAp adsorbent molecule. The FT-IR analyses showed all typical adsorption bands of hydroxyapatite (HAp), apatitic tricalcium phosphate (TCPa) and apatitic octacalcium phosphate (OCPa), thus verifying that the synthesized powders were certainly hydroxyapatite, apatitic tricalcium phosphate and apatitic octacalcium phosphate.

Fig.(2) shows the XRD patterns of the nano-powdered HAp, TCPa and OCPa materials. All reflections of XRD observed for the synthetic HAp, TCPa and OCPa include the characteristic plane reflections at 2Θ = 25° to 44°, are corresponding well to those expected from the HAp, TCPa and OCPa nano-powders structures. The characteristic plane reflections at 2Θ = 10.8° and 23° for HAp and TCPa reflections and not detected for OCPa, revealing that the synthesized OCPa consists of a single OCPa crystalline phase. While, there are reflections appeared at 2Θ = 18° for both TCPa and OCPa powders and not detected for HAp powder, these reflections indicate excess OH and $PO_4$ groups that existed in the TCPa and OCPa powders and not existed in HAp powder. In addition, Fig.(2) indicates that the synthesized HAp, TCPa and OCPa samples are in poor crystalline form which increases their efficiency in the process of absorption, this is manifested by Stötzel *et al*., (2009) which stated that hydroxyapatite powders were used to remove various metal ions from aqueous solution, the ion adsorption capacity of hydroxyapatite increased with decreasing crystallinity and increasing specific surface area.

The XRD patterns were compatible with FT-IR spectra with respect the appearance of excess $OH^-$ and $PO_4^{-3}$ groups in TCPa and OCPa powders and not appeared in the HAp powder. Also, The XRD patterns and FT-IR spectra indicated that HAp, TCPa and OCPa nano-powders were formed in these samples.

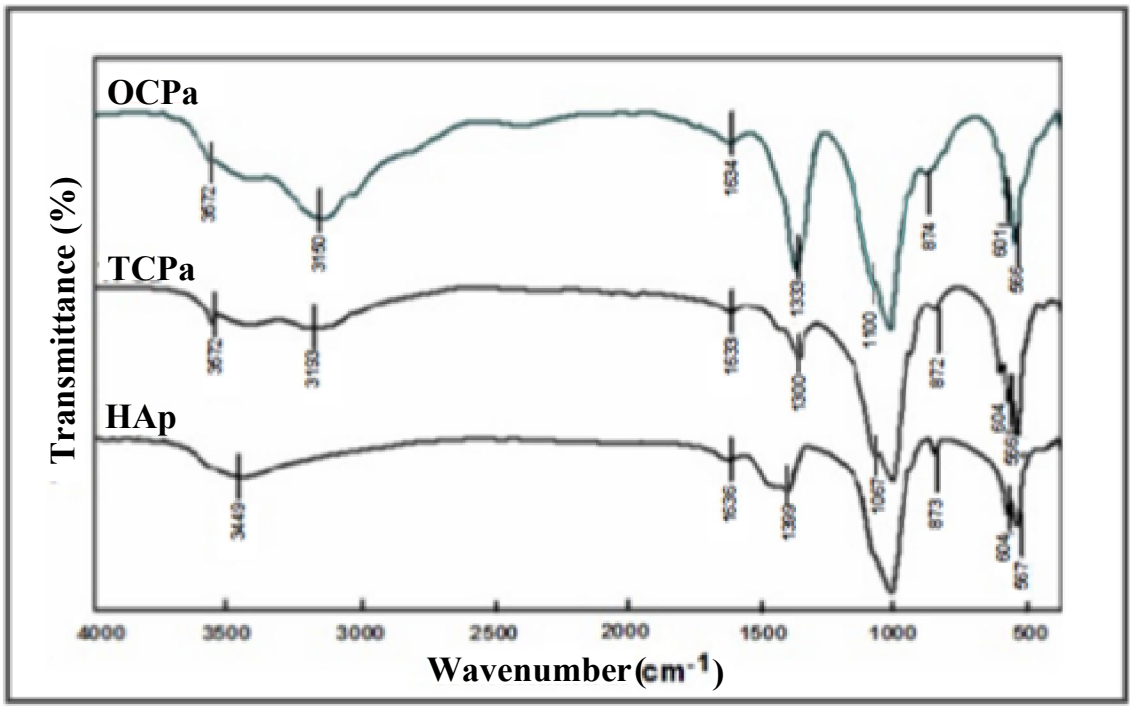


**Fig. 1:** FTIR spectra of the synthesized hydroxyapatite, apatitic tricalcium phosphate and apatitic octacalcium phosphate.

The transmission electron microscopy was used to examine both hydroxyapatite (HAp), apatitic tricalcium phosphate (TCPa) and apatitic octa calcium phosphate (OCPa) nano-powders crystallites. The TEM

micrographs of the synthesized HAp, TCPa and OCPa nano-powders are shown in Fig.(3). The powders exhibited no serious aggregation. The mean crystallite sizes of the particles for HAp, TCPa and OCPa are about (30–40nm width and 70–90nm length), (25–50nm width and 30–40nm length) and (3–5nm width and 5–7nm length), respectively. The microstructure of both HAp, TCPa and OCPa was observed to be almost a needle shaped particles for both hydroxyapatite and apatitic tricalcium phosphate, while being fine shaped particles for apatite cocta calcium phosphate. The needle shaped of the HAp and TCPa adsorbents particles is expected to be more efficient for Fe(II) adsorption process than OCPa adsorbent. In this work, organic solvent, was used to replace water in the system because it can reduce the two major factors that cause the agglomeration of nano-powders when drying from aqueous solutions; one factor is the capillary pressure between the adjacent particles due to the evaporation of water and the other factor is the hydrogen bond originating from the water molecules on the surface of adjacent particles.

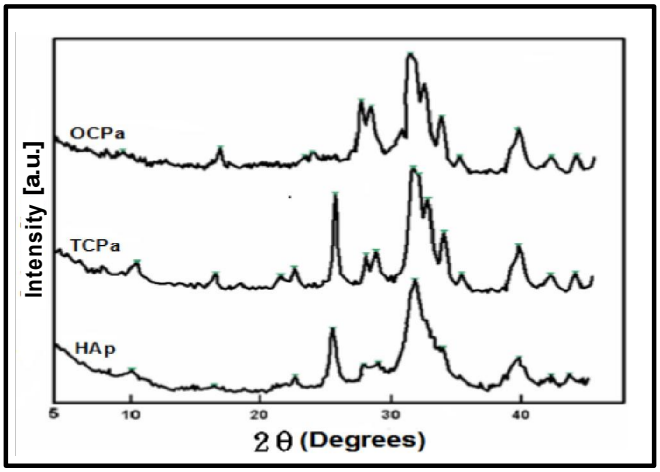


**Fig. 2:** The XRD patterns of HAp, TCPa and OCPa nano-powders.

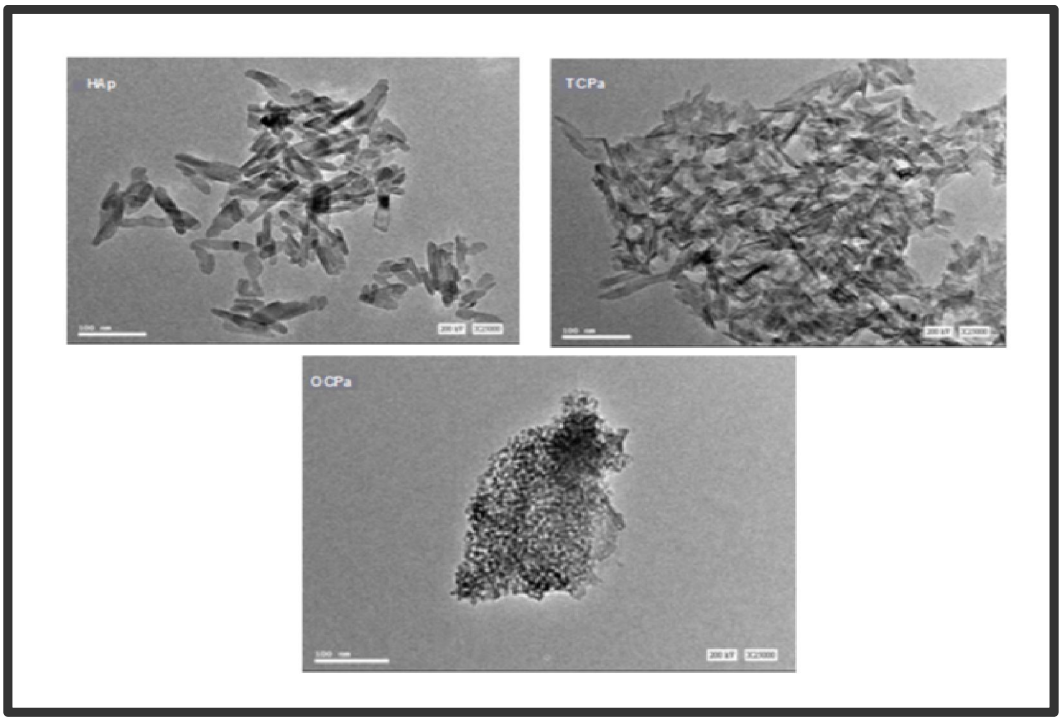


**Fig. 3:** TEM images of the synthesized HAp, TCPa and OCPa nano-powders dried at 80°C.

*Effect of pH on Fe(II) adsorption:*

It is well known that the pH of the adsorption medium represents the most critical parameter affecting the adsorption process in the removal of Fe(II) by the adsorption method; this is due to the effect of the charges of

adsorbate and adsorbent in the pH of solution. The adsorption of Fe(II) by HAp, TCPa and OCPa nano-powders was studied at different initial pH ranging between 3 and 6, contact time 60min, dosage 0.1g, initial concentration 40mg/L and 60ºC. The results are shown in Fig.(4). A maximum sorption capacity (SC) was observed at pH 6. It is apparent from Fig.(4) that the pH has significant effect on the SC of both TCPa and Hap nano-powders, but in case of OCPa, a slight decline is observed with increasing pH of the medium, as TCPa nano-powder possessed higher sorption capacity than those of HAp and OCPa nano-powders at all pH ranges studied.

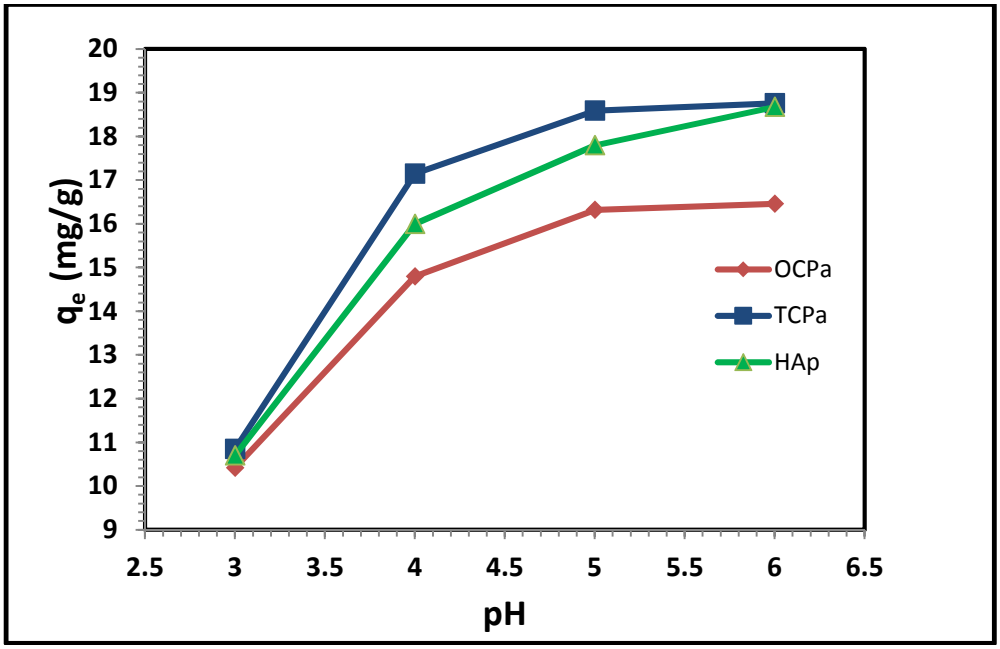


**Fig. 4:** Effect of pH on Fe(II) adsorption by HAp, TCPa and OCPa nano-powders at given conditions; contact time 60min, dosage 0.1g and initial concentration 40mg/L at 60°C.

*Effect of contact time on Fe(II) adsorption:*

The sorption of Fe(II) ions was carried out at different times ranging from 10-60min, pH6 and 60ºC. About 0.1g of the adsorbent was mixed with 50ml of the Fe(II) solution having the initial Fe(II) concentration 40mg/L. Fig.(5) shows the effect of contact time on the adsorption of the Fe(II) by HAp, TPCa and OCPa nano-powders. A rapid kinetic reaction of Fe(II) removal by the HAp, TPCa and OCPa nano-powders adsorbents occurred within the first 30min and the adsorption equilibrium of Fe(II) was achieved after 60min and no remarkable changes were observed for longer contact times. As evidenced from Fig.(5), the sorption capacity (SC) of all the sorbents reached saturation at 60min. Hence, 60min is fixed as the contact time. The SC at 60min contact time of HAp, TCPa and OCPa nano-powders was found to be 18.68, 18.76 and 16.46mg/g, respectively.

*Effect of HAp, TCPa and OCPa nano-powders dosages on Fe(II) adsorption:*

The adsorption of Fe(II) by HAp, TCPa and OCPa nano-powders was studied at different adsorbent dosages ranging from 0.05 to 0.3g, pH 6, contact time 60min, initial Fe(II) concentration 40mg/L and 60ºC. Fig.(6) shows the adsorption capacity ($q_e$) of Fe(II) as a function of HAp, TCPa and OCPa nano-powders dosages. The plot of adsorption capacity revealed that the adsorption capacity was low at dosages 0.05g and progressively increased at dosages that start from 0.1g. Many factors can contribute to this adsorbent concentration effect. The most important factor is that adsorption sites remain unsaturated during the adsorption process. It is readily understood that the number of available adsorption sites increases with the increase of the adsorbent dosage and this, therefore, results in the increasing extent of Fe(II) adsorption. In other words, the adsorption increases with the increase in the mass of sorbent, this is because at the higher dosage of sorbent due to increased surface area, more adsorption sites are available causing higher removal of Fe(II).

*Effect of initial Fe(II) concentration on the adsorption process:*

The adsorption of Fe(II) by the HAp, TCPa and OCPa nano-powders adsorbents was studied at different Fe(II) initial concentrations ranging from 10 to 40mg/L, pH 6, contact time 60min, dosage 0.1g and 60ºC.

Fig.(7) shows the effect of Fe(II) initial concentration on the adsorption processes. It is evident that the $q_e$ values increase with the increase in the initial Fe(II) concentrations. However, there is no distinct difference in $q_e$ values with the initial Fe(II) concentration lower than 20mg/l, which indicates that the adsorption reaches saturation at high Fe(II) concentration as the adsorbent offers a limited number of surface binding sites. In other words, as shown in Fig.(7), when the initial Fe(II) concentration increased from 20 to 40mg/L, the uptake capacity of the HAp, TCPa, and OCPa adsorbents increased from 9.99 to 18.68mg/g, from 9.97 to 18.76mg/g and from 9.98 to 16.46mg/g, respectively. Thus, higher initial concentration provides an important driving force to overcome all mass transfer resistance of the pollutant between the aqueous and solid phases, thus increases the uptake (Aksu and Tezer, 2005).The maximum equilibrium $q_e$ values obtained for HAp, TCPa, and OCPa are 18.68, 18.76 and 16.46mg/g, respectively (Fig.8).

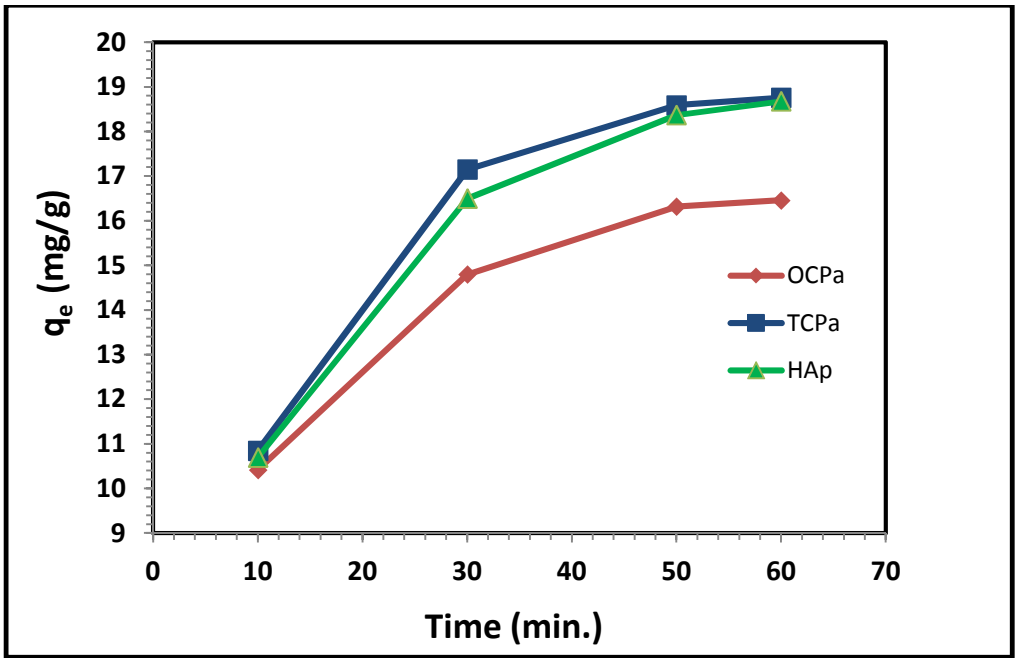


**Fig. 5:** Effect of contact time on Fe(II) adsorption by HAp, TCPa and OCPa nano-powders at given conditions; pH 6, dosage 0.1g and initial concentration 40mg/L at 60°C

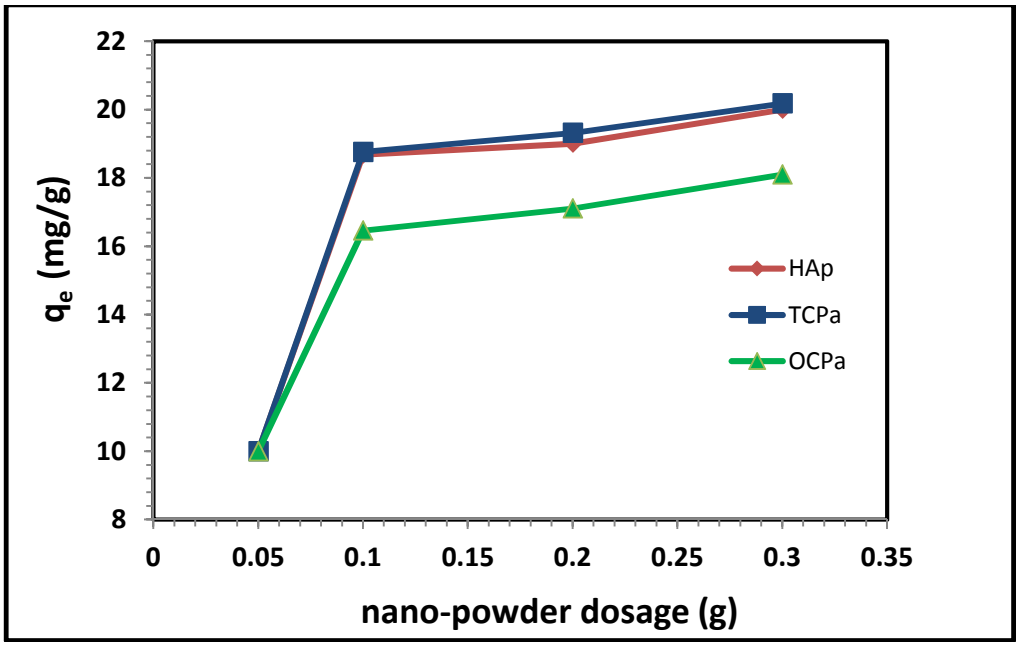


**Fig. 6:** Effect of HAp, TCPa and OCPa nano-powders dosage on Fe(II) adsorption at given conditions;pH 6, contact time 60min and initial concentration 40mg/L at 60°C.

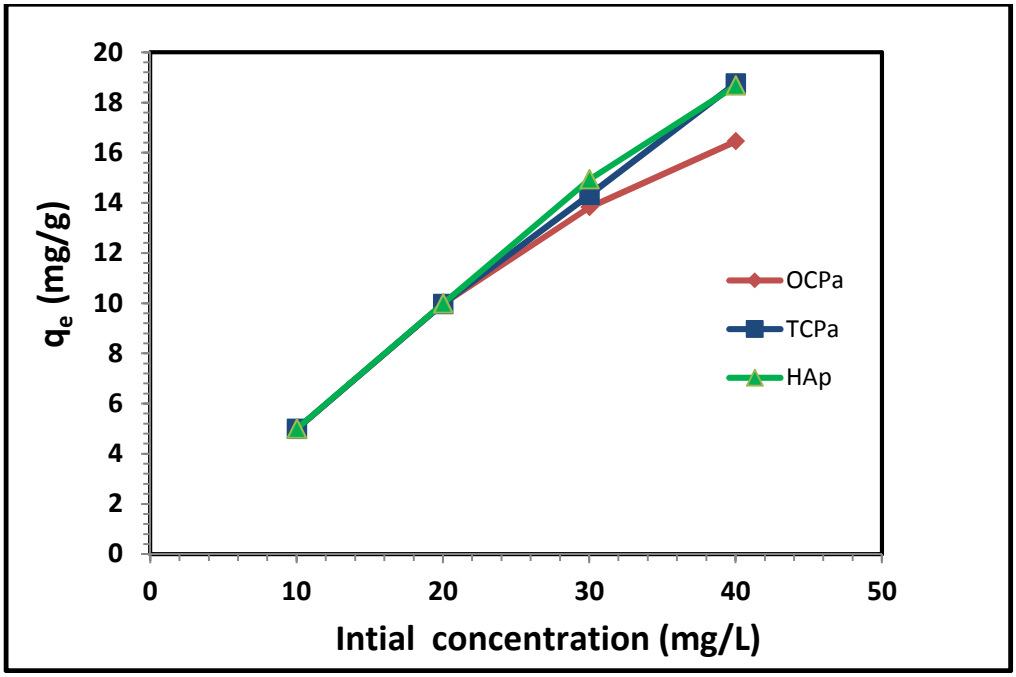


**Fig. 7:** Effect of Fe(II) initial concentration on the adsorption processes by HAp, TCPa and OCPa nano-powders at given conditions; pH 6, contact time 60min, dosage 0.1g at 60°C.

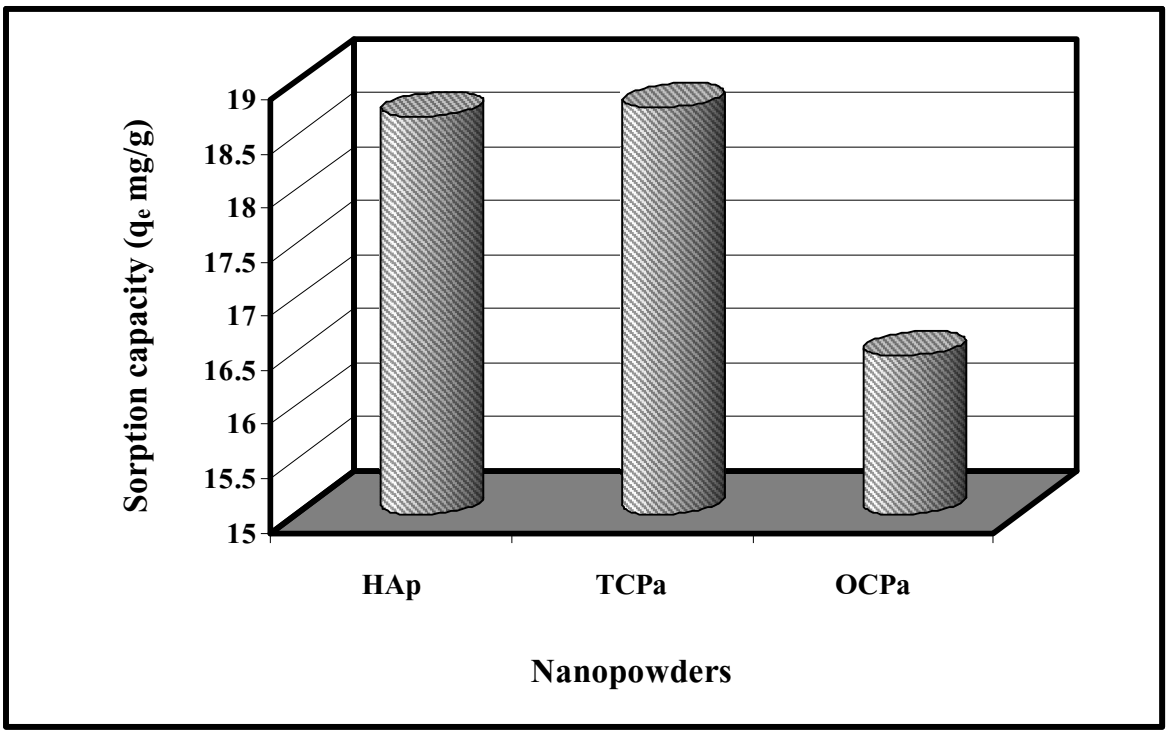


**Fig. 8:** The Sorption capacities of HAp, TCPa and OCPa nano-powders.

*Effect of temperature on the adsorption process:*

To study the effect of this parameter on the uptake of Fe(II) ions by nano-powdres HAp, TCPa and OCPa adsorbents, the adsorption was conducted at different temperatures ranging from 20 to 60°C, pH6, contact time 60min, dosage 0.1g and initial concentration 40mg/L. Fig.(9) illustrates the relationship between temperature and the amount of Fe(II) ions adsorbed onto HAp, TCPa and OCPa adsorbents. As seen in Fig.(9), the

adsorption of Fe(II) on HAp, TCPa and OCPa adsorbents slightly increased when temperature was increased from 20 to 60ºC. However, the magnitude of increase is typical for TCPa and HAp while being less for OCPa.The increase in the equilibrium sorption of Fe(II) with temperature indicates that Fe(II) ions removal by adsorption on HAp, TCPa and OCPa adsorbents is favored by high temperature. This may be a result of increase in the mobility of the Fe(II) ion with temperature. An increasing number of molecules may also acquire sufficient energy to undergo an interaction with active sites at the surface. Furthermore, increasing temperature may produce a swelling effect within the internal structure of the adsorbent enabling metal ions to penetrate further (Dôgan and Alkan, 2003).

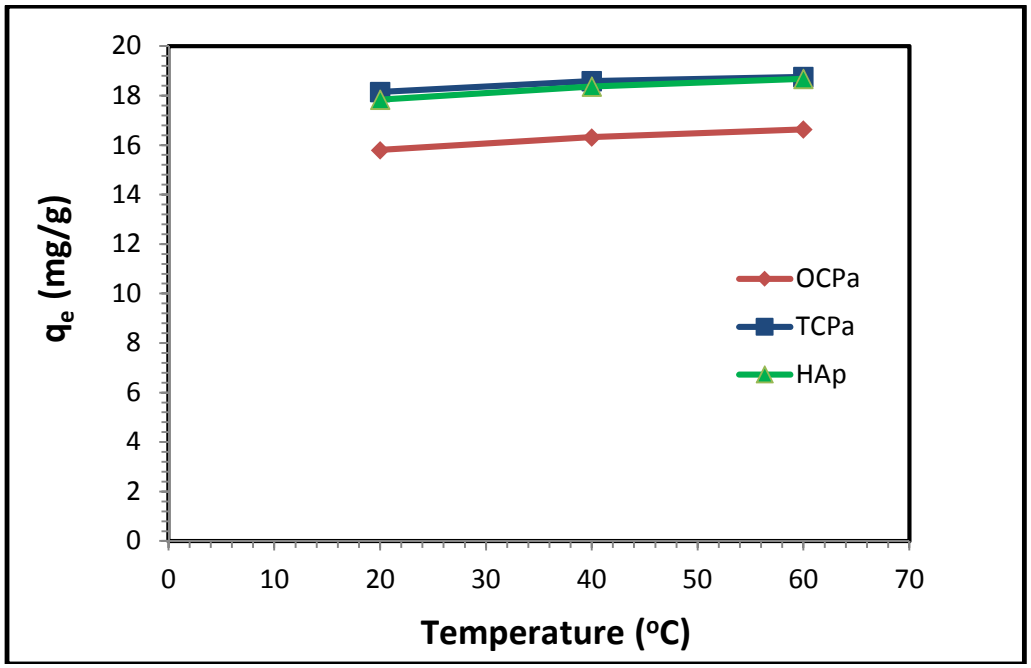


**Fig. 9:** Effect of temperature on the adsorption processes of Fe(II) by HAp, TCPa and OCPa nano-powders at given conditions; pH 6, contact time 60min, dosage 0.1g and initial concentration 40mg/L.

*Adsorption isotherms:*

Adsorption of the equilibrium data is important to develop an equation which accurately represents the result and which could be used for design purpose (Aksu, 2002). Several isotherms equations have been used for the equilibrium modeling of adsorption systems, among them, the Langmuir (1918) and Freundlich (1906) equilibrium isotherm models were used to describe the adsorption equilibrium of Fe(II) on HAp, TCPa and OCPa nano-powders in solution at different constant temperatures.

1) The equilibrium data for metal cation ($Fe^{2+}$) over the concentration range from 10-40mg/L have been correlated with the Langmuir isotherm model which is used to describe the adsorption equilibrium of Fe(II) by HAp, TCPa and OCPa nano-powders in solution at different temperatures. Also, Langmuir isotherm model is one of the most popular isotherm models due to its simplicity and it is valid for monolayer adsorption onto a surface containing a finite number of identical sites, and it is in good agreement with experimental data. The Langmuir isotherm equation can be expressed as;

$$\frac{C_e}{q_e} = \frac{1}{Q_o} + \frac{C_e}{KQ_o} \quad (2)$$

Equation (2) can be written as follow;

$$q_e = \frac{Q_o K C_e}{1 + K C_e} \quad (3)$$

$$\frac{1}{q_e} = \frac{1}{Q_o} + \frac{1}{Q_o K C_e} \quad (4)$$

Where, $C_e$ is the equilibrium concentration of metal in solution (mg/L), $q_e$ is the amount absorbed at equilibrium onto nano-powder adsorbent (mg/g), $Q_o$ and $K$ are Langmuir constants related to sorption capacity and sorption

energy, respectively. Maximum sorption capacity *($Q_o$)* represents monolayer coverage of sorbent with sorbate and *K* represents enthalpy of sorption and should vary with temperature. A linear plot is obtained when *$1/q_e$* is plotted versus*$1/C_e$* over the entire concentration range of metal ion investigated (Fig.10).

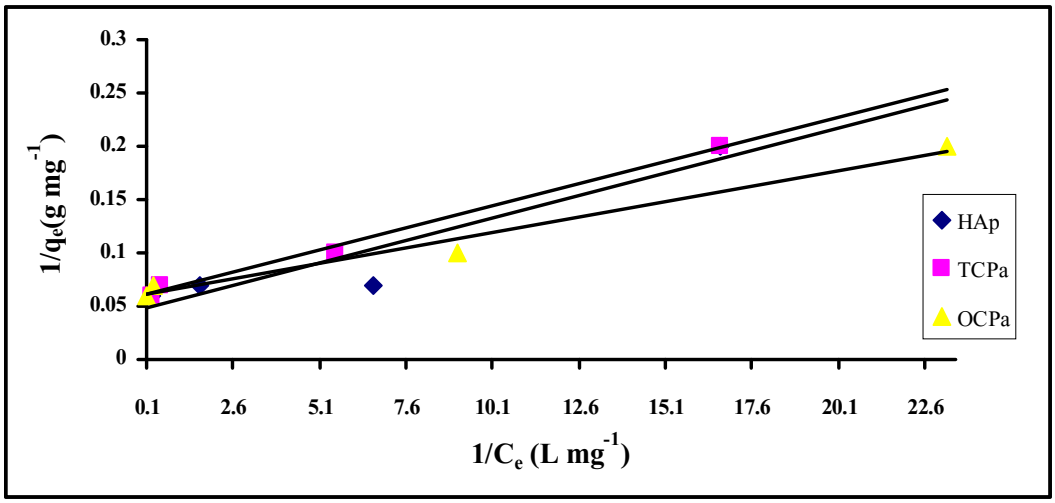


**Fig. 10:** The Langmuir isotherm plot for Fe(II) adsorption by HAp, TCPa and OCPa nano-powders at given conditions; pH 6, contact time 60min, dosage 0.1g and initial concentration 40mg/L at 60°C.

2) The Freundlich sorption isotherm, one of the most widely used mathematical descriptions, usually fits the experimental data over a wide range of concentrations. This isotherm gives an expression encompassing the surface heterogeneity and the expositional distribution of active sites and their energies. It assumes that the adsorption process occurs on heterogeneous surfaces and the adsorption capacity is related to the concentration of Fe(II) at equilibrium. So, the Freundlich adsorption isotherms is applied to the removal of Fe(II) on nano-powders of HAp, TCPa and OCPa adsorbents (Fig.11). The Freundlich model is generally represented as follows;

$$q_e = k_f C_e^{1/n} \quad (5)$$

Where, $q_e$ is the amount of metal ion sorbed at equilibrium per gram of adsorbent (mg/g), $C_e$ is the equilibrium concentration of metal ion in the solution (mg/L), $k_f$ and $n$ are the Freundlich model constants (Malkoc and Nuhŏglu, 2003 and, Kadirvelu *et al*., 2001). Freundlich parameters, the maximum adsorption capacity ($k_f$) as mg/g and the affinity value ($n$), were determined by plotting $\ln q_e$ versus $\ln C_e$ (Fig.11). The constant $n$ is the empirical parameter related to the intensity of adsorption, which varies with the heterogeneity of the material. When *1/n* values are in the range $0.1 < 1/n < 1$, the adsorption process is favorable (Vazquez *et al*., 2007). The numerical value of $1/n < 1$ indicates that adsorption capacity is only slightly suppressed at lower equilibrium concentrations. This isotherm does not predict any saturation of the sorbent by the sorbate; thus infinite surface coverage is predicted mathematically, indicating multilayer adsorption on the surface (Hasany *et al*., 2002). For fitting the experimental data, the Freundlich model was linearized as follows;

$$\ln q_e = \ln k_f + (1/n) \ln C_e \quad (6)$$

Figures 10 and 11 show the fitting plots of Langmuir and Freundlich adsorption isotherms of Fe(II) onto HAp, TCPa and OCPa nano-powders at 60°C, respectively. Table (1) summarizes the constants of Freundlich and Langmuir isotherms obtained from the slope and intercept of the plots at the different constant temperatures. Most of the $R^2$ values exceed 0.9 for Langmuir model, suggesting that the Langmuir model closely fitted the experimental results.

With respect to the coefficients of the Langmuir model, the values of *K* were (5.8, 11.02 and 35.13L/mg), (6.89, 13.64 and 19.52L/mg) and (11.09, 12.68 and 23.12L/mg) for HAp, TCPa and OCPa at 20, 40 and 60°C, respectively. The value of *K* increases with increasing temperature, revealing that the adsorption capacity of Fe(II) onto HAp, TCPa and OCPa increases with increasing temperature. The results implied also that the affinity of binding sites for Fe(II) increase with increasing temperature. These results showed that the adsorption of Fe(II) onto the HAp, TCPa and OCPa nano-powders is correlated well with the Langmuir equation as

compared to Freundlich equation under the concentration range studied, as shown by the $R^2$ values shown in (Table 1).

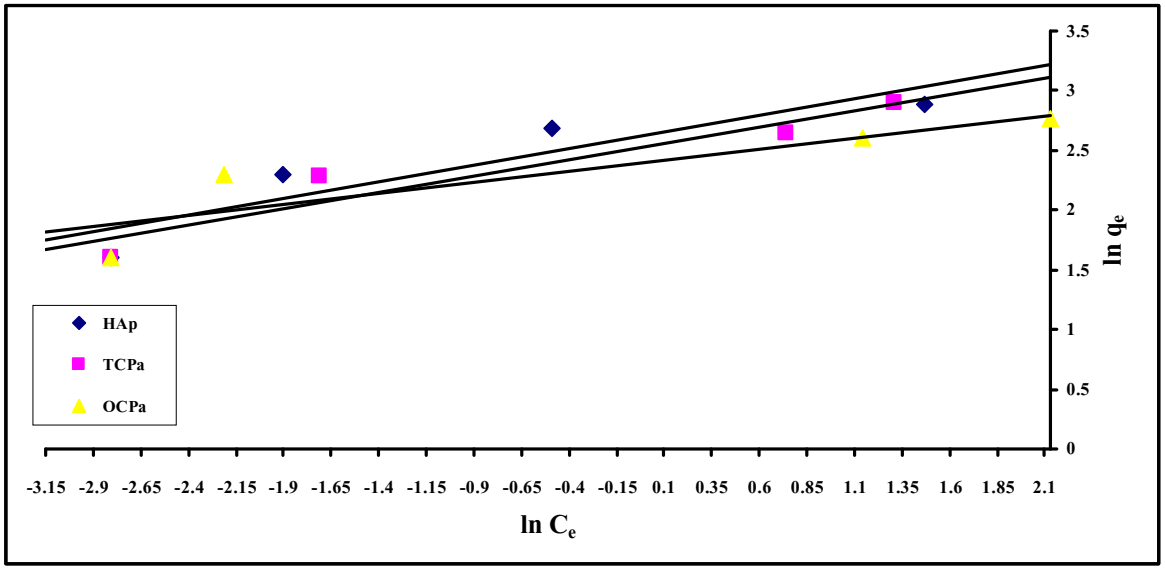


**Fig. 11:** The Freundlich isotherm plot for Fe(II) adsorption by HAp, TCPa and OCPa nano-powders at given conditions; pH 6, contact time 60min, dosage 0.1g and initial concentration 40mg/L at 60°C.

**Table 1:** The adsorption parameters derived from Freundlich and Langmuir isotherms for Fe(II) adsorption on the HAp, TCPa and OCPa nano-powders.

| Sorbents | Temp. (K) | Langmuir isotherm | | | Freundlich isotherm | | | |
|---|---|---|---|---|---|---|---|---|
| | | $q_e$ (mg/g) | *K* (L/mg) | $R^2$ | 1/n | n | $k_f$ (L/mg) | $R^2$ |
| HAp | 293 | 19.61 | 5.80 | 0.99 | 0.28 | 3.62 | 0.06 | 0.83 |
| | 313 | 21.10 | 11.02 | 0.96 | 0.24 | 4.11 | 0.08 | 0.78 |
| | 333 | 18.98 | 35.13 | 0.99 | 0.21 | 4.72 | 0.10 | 0.79 |
| TCPa | 293 | 17.06 | 6.89 | 0.99 | 0.27 | 3.68 | 0.04 | 0.91 |
| | 313 | 17.45 | 13.64 | 0.98 | 0.24 | 4.22 | 0.06 | 0.78 |
| | 333 | 17.67 | 19.52 | 0.98 | 0.23 | 4.40 | 0.07 | 0.87 |
| OCPa | 293 | 15.82 | 11.09 | 0.97 | 0.18 | 5.51 | 0.02 | 0.82 |
| | 313 | 16.78 | 12.68 | 0.89 | 0.18 | 5.71 | 0.03 | 0.78 |
| | 333 | 16.64 | 23.12 | 0.94 | 0.15 | 6.67 | 0.04 | 0.80 |

The values of $k_f$ increase with increasing temperature, revealing that the adsorption capacity of Fe(II) onto HAp, TCPa and OCPa nano-powders increase with the increases in the temperature. Like $k_f$, the n-values increase with increasing temperature. The highest values of *n* are 6.67, 4.72 and 4.40 for OCPa, HAp and TCPa, respectively, at 60°C; this represents favorable adsorption at the higher temperature. If the *n* is below one, then the adsorption is chemical process; otherwise, the adsorption is physical process (Jiang *et al*., 2002). All values of n exceed one, suggesting the adsorption of Fe(II) onto HAp, TCPa and OCPa is physical process. On the other hand, the Freundlich exponent of 1/*n* gives information about surface heterogeneity and surface affinity for the solute. The Freundlich exponent *1/n* between [(0.21 and 0.28), (0.23 and 0.27) and (0.15 and 0.18)] for the HAp, TCPa and OCPa, respectively, indicates favorable adsorption and a high affinity of the nano-powders for Fe(II) adsorption. Gemeay, (2002) suggested that the higher value of *1/n* corresponds the greater heterogeneity of the adsorbent surface. Thus, the degree of heterogeneity of the HAp, TCPa and OCPa surfaces decreases with the increase in the temperatures (as in table 1).

Evidently, variation of the adsorption parameters, derived from Langmuir and Freundlich models, with increasing temperature indicated that the adsorption process is mainly physical in nature with a partial transformation to chemical adsorption with increasing temperature from 40 to 60°C; this kind of transition takes place at the intermediate temperature range (20-60°C) used in this study, while at the higher temperature range (more than 60°C) chemical adsorption may become more favorable.

Both the Langmuir and Freundlich models suggested that the adsorption capacity increases with increasing temperature for the three powders, revealing that the adsorption is endothermic (Wu, 2007). At the optimum conditions for adsorption processes for Fe(II) onto the HAp, TCPa and OCPa nano-powders adsorbents, the correlation factors (R) for Langmuir isotherm (Table 1) confirms good agreement between both theoretical adsorption capacity results (18.98, 17.67 and 16.64mg/g) and our experimental adsorption capacity

results(18.68, 18.76 and 16.46mg/g). It is clear that the Langmuir isotherm has best fitted for the sorption of Fe(II) on nano-powders of HAp, TCPa and OCPa adsorbents.

Generally, the selectivity of each HAp or TCPa or OCPa adsorbent towards divalent metal cations is a result of the ion exchange process with $Ca^{2+}$ ions. Ionic radius of $Fe^{2+}$ (0.645Å) slightly differs from that of $Ca^{2+}$ (0.99Å), and it can be substitute $Ca^{2+}$ in HAp or TCPa or OCPa crystal lattice.

Mechanistically, ion removal from solution by apatites (HAp, TCPa and OCPa) can occur by two mechanismsas in Scheme (1). Firstly, apatite could provide phosphorous by dissolution in acidic environments (Equations 1, 2 and 3). These phosphates can react with the metal ions ($Fe^{2+}$) to precipitate low soluble metal phosphate crystals with an apatitic structure according to equations **(**4, 5 and 6).

$Ca_{10}(PO_4)_6(OH)_2+14H^+ \rightarrow 10Ca^{2+} +6H_2PO_4^- +2H_2O$ (1)
$Ca_9(HPO_4)(PO_4)_5(OH)+12H^+ \rightarrow 9Ca^{2+} +6H_2PO_4^- +H_2O$ (2)
$Ca_8(PO_4)_4(HPO_4)_2.5H_2O+10H^+ \rightarrow 8Ca^{2+} +6H_2PO_4^- +5H_2O$ (3)
$10Fe^{2+} +6H_2PO_4^- +2H_2O \rightarrow Fe_{10}(PO_4)_6(OH)_2+14H^+$ (4)
$9Fe^{2+} +6H_2PO_4^- +H_2O \rightarrow Fe_9(HPO_4)(PO_4)_5(OH)+12H^+$ (5)
$8Fe^{2+} +6H_2PO_4^- + 5H_2O \rightarrow Fe_8(PO_4)_4(HPO_4)_2.5H_2O+10H^+$ (6)

**Scheme 1:** Reaction mechanism of Fe(II) adsorption by HAp, TCPa and OCPa nano-powders (modified after Zhang *et al*., 1998).

In a second ion exchange theory, metal ions that are adsorbed to the surface of the apatite particle will substitute $Ca^{2+}$ ions from the apatite lattice by a diffusion process as in scheme 2 (Equations 1, 2 and 3).This reaction mechanism corresponds to equimolar exchange of iron and calcium for HAp, TCPa and OCPa, respectively, where *x* can vary from 0 to 10, from 0 to 9 and from 0 to 8 for HAp, TCPa and OCPa, respectively, depending on the reaction time and experimental conditions.

$Ca_{10}(PO_4)_6(OH)_2+xFe^{2+} \rightarrow (Ca_{10-x})Fe_x(PO_4)_6(OH)_2+xCa^{2+}$ (1)
$Ca_9(HPO_4)(PO_4)_5(OH)+xFe^{2+} \rightarrow (Ca_{9-x})Fe_x(HPO_4)(PO_4)_5(OH)+xCa^{2+}$ (2)
$Ca_8(PO_4)_4(HPO_4)_2.5H_2O+xFe^{2+} \rightarrow (Ca_{8-x})Fe_x(PO_4)_4(HPO_4)_2 \cdot 5H_2O+xCa^{2+}$ (3)

**Scheme 2:** Reaction mechanism of Fe(II) adsorption by HAp, TCPa and OCPa nano-powders (modified after Takeuchi and Arai 1990)

*Field study:*

The suitability of HAp, TCPa and OCPa nano-powders was tested with groundwater samples collected from the study area. About 0.1g of sorbent was added to 50mL of water sample and the contents were shaken at constant time (120min.) at room temperature. The results are presented in Table (2). There is a significant reduction in the level of Fe(II). It is evident from the results that HAp, TCPa andOCPa can be effectively employed for removing Fe(II) from water as follows;

**Table 2:** Field trial results for adsorption process of $Fe^{2+}$ (mg/L) onto HAp, TCPa and OCPa nano-powders.

| Before treatment | After treatment | | |
|---|---|---|---|
| | HAp | TCPa | OCPa |
| $Fe^{2+}$(3.78 mg/L) | 0.08 mg/L | 0.06 mg/L | 0.10 mg/L |
| Removal (%) | 97.9 | 98.4 | 97.4 |

*Conclusions:*

The present investigation showed that the HAp, TCPa and OCPa nano-particles are effective adsorbents for the removal of $Fe^{2+}$ ions from aqueous solutions. The adsorption process is a function of pH, contact time, adsorbent dosage, initial $Fe^{2+}$ concentration and temperature. The efficiency of $Fe^{2+}$ adsorption increases with increasing adsorbent dosage and temperature. Isotherm studies indicate that the Langmuir model fits the experimental data better than Freundlich model. The maximum adsorption capacities $q_e$ values for HAp, TCPa and OCPa nano-particles are 18.68, 18.76 and 16.46mg/g, respectively. The main advantage of HAp, TCPa and OCPa are biocompatible and hence could be utilized for field applications in water treatment despite their effect on quality of water.

**References**

Aksu, Z., 2002. Determination of the equilibrium, kinetic and thermodynamic parameters of the batch biosorption of nickel(II)ions onto Chlorella veulgaris. Process Biochem., 38: 89-99.

Aksu, Z., A. Calik, A.Y. Dursun and Z. Demircan, 1999. Biosorption of iron(III)-cyanide complex anions to Rhizopusarrhizus: Application of adsorption isotherms. Process Biochem., 34: 483-491.

Aksu, Z. and S. Tezer, 2005. Biosorption of reactive dyes on the green alga Chlorella veulgaris. Process Biochem., 40: 1347-1361.

Aydin, F.A. and M. Soylak, 2007. A novel multi-element co-precipitation technique for separation and enrichment of metal ions in environmental samples. Atlanta, 73: 134-141.

Cazalbou, S., D. Eichert, X. Ranz, C. Drout, C. Combes, M.F. Harmand and C. Rey, 2005. J. Mater. Sci. Mater. Med., 16: 405-409.

Chen, X., J.V. Wright, J.L. Conca and L.M. Peurrung, 1997. Effects of pH on heavy metal sorption on mineral apatite. Environ. Sci. Technol., 31: 624-631.

Destainville, A., E. Champion, D. Bernache-Assollant and E. Laborde, 2003. Synthesis, characterization and thermal behavior of apatitic tricalcium phosphate. Materials Chemistry and Physics, 80: 269-277.

Dôgan, M. and M. Alkan, 2003. Adsorption kinetics of methyl violet onto perlite. Chemosphere, 50: 517-528.

Elliott, J.C., 1994. Structure and Chemistry of the Apatite's and Other Calcium Orthophosphates. Elsevier, Amsterdam.

El-Shafey, E., M. Pichugin and A. Appleton, 2002. Application of a carbon sorbent for the removal of cadmium and other heavy metal ions from aqueous solution. J. Chem. Technol. Biotechnol., 77: 429-436.

Freundlich, H.M.F., 1906.Adsorption in solution. Phys. Chem. Soc., 40: 1361-1368.

Gemeay, A.H., 2002. Adsorption characteristics and the kinetics of the cation exchange of rhodamine-6G with $Na^{+}$-montmorillonite. J. Colloid Interface Sci., 251: 235-241.

Hasany, S.M., M.M. Saeed, M. Ahmed and J. Radioanal, 2002. Sorption and thermodynamic behavior of zinc(II)-thiocyanate complexes onto polyurethane foam from acidic solutions. Nucl. Chem., 252: 477-484.

Jiang, J.Q., C. Cooper and S. Ouki, 2002. Comparison of modified montmorillonite adsorbents. Part I. Preparation, characterization and phenol adsorption. Chemosphere, 47: 711-716.

Kadirvelu, K., K. Thamaraiselvi and C. Namasivayam, 2001. Adsorption of nickel (II) from aqueous solution onto activated carbon prepared from coirpith. Sep. Purif. Technol., 24: 497-505.

Komath, M. and H.K. Varma, 2003. Development of a fully injectable calcium phosphate cement for orthopedic and dental applications. Bull. Mater. Sci., 26(4): 415-422. Indian Academy of Science.

Krestou, A., A. Xenidis and D. Panias, 2004. Mechanism of aqueous uranium (VI) uptake by a natural zeolitic tuff. Miner. Eng., 16: 1363-1370.

Langmuir, I., 1918. The adsorption of gasses on plane surfaces of glass, mica and platinum. J. Am. Chem. Soc. 40: 1361-1368.

Laperche, V., S.J. Traina, P. Gaddam, T.J. Logan and J.A. Ryan, 1996. Chemical and mineralogical characterizations of Pb in a contaminated soil: reactions with synthetic apatite. Environ. Sci. Technol., 30: 3321-3326.

Lebugle, A., E. Zahidi and G. Bonel, 1986. Effect of structure and composition on the thermal decomposition of calcium phosphates (Ca/P= 1.33). Reactivity of Solids, 2(1-2): 151-161.

Ma, Q.Y., S.J. Traina, T.J. Logan and J.A. Ryan, 1993. In situ lead immobilization by apatite. Environ. Sci. Technol., 27: 1803-1810.

Ma, Q.Y., S.J. Traina, T.J. Logan and J.A. Ryan, 1994. Effects of aqueous Al, Cd, Cu, Fe(II), Ni, and Zn on Pb immobilization by hydroxyapatite. Environ. Sci. Technol., 28: 1219-1228.

Malkoc, E. and Y. Nuhŏglu, 2003. The removal of chromium (VI) from synthetic wastewater by Ulothrixzonata. Fresenius Environ. Bull., 12: 376-381.

Mavropoulos, E., A.M. Rossi, A.M. Costa, C.A. Perez, J.C. Moreira and M. Saldanha, 2002. Studies on the mechanisms of lead immobilization by hydroxyapatite. Environ. Sci. Technol., 36: 1625-1629.

Mobasherpour, I., M.B. Soulati Heshajin, A. Kazemzadeha and M. Zakeri, 2007. Synthesis of nano-crystalline hydroxyapatite by using precipitation method. J. of Alloys and Compounds, 430: 330-333.

Moore, D.M. and R.C. Reynolds, 1989. X-ray diffraction and the identification and analysis of clay minerals. Oxford University Press (OUP), Oxford, U.K. 332p.

Nzihou, A. and P. Sharrock, 2002. Calcium phosphate stabilization of fly ash with chloride extraction. Waste Management, 22: 235-239.

Okamoto, Y., Y. Nomura and K. Iwamaru, 2000. High preconcentration of ultra-trace metal ions by liquid-liquid extraction using water/oil/water emulsions as liquid surfactant membranes. Microchem. J., 65: 341-346.

Safavi, A. and H. Abdollahi, 1999. Speciation of Fe(II) with chromagenic mixed reagents by principal-component regression. Microchem. J., 63: 211-217.

Sarzanini, C., O. Abolino and E. Mentastri, 2001. Flow-injection preconcentration and electrothermal atomic absorption spectrometry determination of manganese in seawater. Anal. Chim., 435: 343-350.

Stötzel, C., F.A. Müllerb, F. Reinert, F. Niederdraenk, J.E. Barralet and U. Gburecka, 2009. Ion adsorption behavior of hydroxyapatite with different crystallinities. Colloids Surfaces B Biointerfaces journal, 74(1): 91-95.

Takeuchi, Y. and H. Arai, 1990. Removal of coexisting $Pb^{2+}$, $Cu^{2+}$, $Cd^{2+}$ ions from water by addition of hydroxyapatite powder. J. Chem. Eng. Jpn., 23: 75-80.

Tanaka, H., M. Futaoka, R. Hino, K. Kandori and T. Ishikawa, 2005. Structure of synthetic calcium hydroxyapatite particles modified with pyrophosphoric acid. J. Colloid Interf. Sci., 283: 609-612.

Vazquez, I., J. Rodrıguez-Iglesias, E. Maranon, L. Castrillon and M. Alvarez, 2007. Removal of residual phenols from coke wastewater by adsorption. J. Hazard. Mater, 147(1-2): 395-400.

Wan, W.S., S. Ngah, A. Ghani and A. Kamari, 2005. Adsorption behaviour of Fe(II) ions in aqueous solution on chitosan and cross-linked chitosan beads. Bioresour. Technol., 96: 443-450.

Wei, M., J.H. Evans, T. Bostromand L. Grondahl, 2003. Synthesis and characterization of hydroxyapatite, fluoride-substituted hydroxyapatite and fluorapatite. J. Mater. Sci. Med., 14(4): 311-320.

Wu, C.H., 2007. Adsorption of reactive dye onto carbon nanotubes: equilibrium, kinetics and thermodynamics. J. Hazard. Mater, 144(1-2): 93-100.

Zhang, P.C., J.A. Ryan and J. Yang, 1998. In vitro soil Pb solubility in the presence of hydroxyapatite. Environ. Sci. Technol., 32(18): 2763-2768.